CHEMISTRY
A EUROPEAN JOURNAL

DOI: 10.1002/chem.200801046

A Phosphotyrosine-Imprinted Polymer Receptor for the Recognition of Tyrosine Phosphorylated Peptides

Marco Emgenbroich,[a] Cristiana Borrelli,[a] Sudhirkumar Shinde,[a] Issam Lazraq,[a] Filipe Vilela,[a] Andrew J. Hall,[a, e] Joakim Oxelbark,[b] Ersilia De Lorenzi,[b] Julien Courtois,[c] Anna Simanova,[c] Jeroen Verhage,[c] Knut Irgum,[c] Kal Karim,[d] and Börje Sellergren*[a]

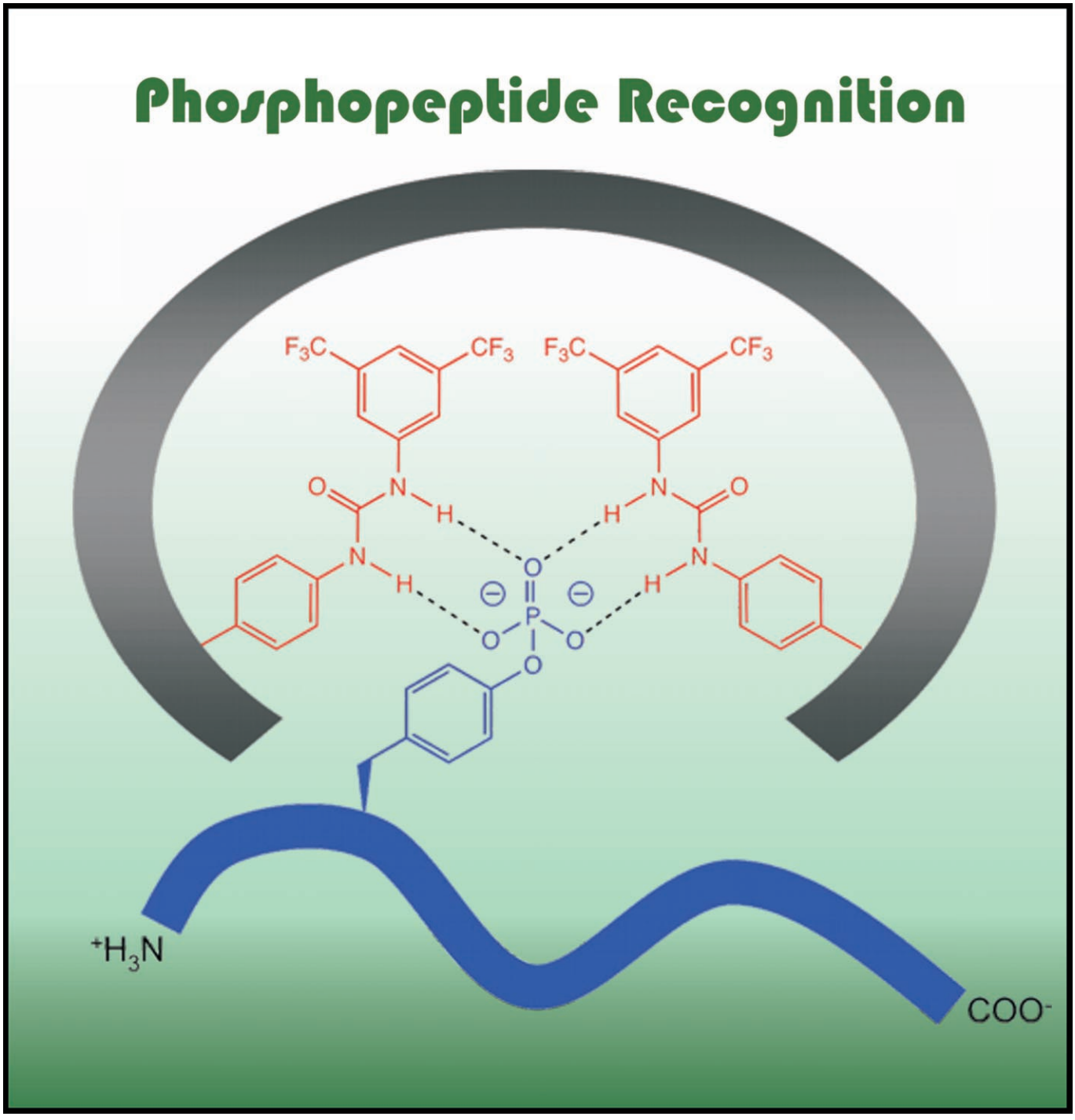

Abstract: Hyperphosphorylation at tyrosine is commonly observed in tumor proteomes and, hence, specific phosphoproteins or phosphopeptides could serve as markers useful for cancer diagnostics and therapeutics. The analysis of such targets is, however, a challenging task, because of their commonly low abundance and the lack of robust and effective preconcentration techniques. As a robust alternative to the commonly used immunoaffinity techniques that rely on phosphotyrosine-(pTyr)-specific antibodies, we have developed an epitope-imprinting strategy that leads to a synthetic pTyr-selective imprinted polymer receptor. The binding site incorporates two monourea ligands placed by preorganization around a pTyr dianion template. The tight binding site displayed good binding affinities for the pTyr template, in the range of that observed for corresponding antibodies, and a clear preference for pTyr over phosphoserine (pSer). In further analogy to the antibodies, the imprinted polymer was capable of capturing short tyrosine phosphorylated peptides in the presence of an excess of their non-phosphorylated counterparts or peptides phosphorylated at serine.

Keywords: antibody mimics · epitome imprinting · molecular recognition · phosphopeptides · proteomics

Introduction

Protein phosphorylation and dephosphorylation is a key regulating mechanism of biological processes and, therefore, is a post-translational modification of profound biological importance.[1] Defects in the function or level of the enzymes carrying out the modification, that is, the kinase/phosphatase switch, have been implicated as the major cause of several diseases, including cancer. Comprehensive mapping of the phosphoproteome is, therefore, an important objective in today's proteomics research.[2–5] In this context, it has proven particularly difficult to obtain a comprehensive view of proteins phosphorylated at tyrosine (Scheme 1).[4] This is because the prefractionation techniques used for this purpose commonly lack the selectivity, sensitivity, and robustness required for reproducibly extracting these low-abundant proteins.[2] An urgent need for alternative affinity techniques has therefore emerged.

In this area, molecularly imprinted polymers could play an important role, thus complementing currently used immunological and chemical methods. Molecular imprinting has resulted in a range of robust polymer-based receptors, predominantly for small lipophilic target molecules.[6,7] The technique entails copolymerization of mono- and bifunctional monomers in the presence of a template, which is thereafter removed to leave sites that can be reoccupied by the template or closely related compounds. Regarding biological receptors, they are distinguished by their robustness and ease of synthesis, which has led to their assessment in a range of molecular-recognition-based applications that target small molecules.

Although molecularly imprinted polymers (MIPs) have proven their value for the enrichment of low-molecular-weight analytes, their use in the enrichment of peptide or protein target molecules has so far met with limited success.[8] Epitope imprinting, which uses shorter peptide sequences that correspond to the N− or C− termini of the target, has, in this context, emerged as a promising strategy.[9–11]

Following this approach to the synthesis of phospho-peptide or protein receptors, we reasoned would require the formation of a tight binding site for the phosphorylated side chain. Binding of this residue should be strong enough to overcome unfavorable secondary interactions and the site should be accessible for protein targets. In a first attempt to meet these requirements, we decided to make use of our recently reported urea-based host monomers[12–14] in combination with an N,O-protected pTyr template (Scheme 2) and to probe the recognition properties on a peptide level. We anticipated that these neutral hydrogen-bond receptors would provide sufficient binding energy while not suffering from the charge-dependent sequence bias commonly observed for positively charged chelating receptors.[15]

[a] Dr. M. Emgenbroich, C. Borrelli, S. Shinde, I. Lazraq, Dr. F. Vilela, Dr. A. J. Hall, Priv. Doz. Dr. B. Sellergren
INFU, Technische Universität Dortmund
Otto Hahn Strasse 6
44221 Dortmund (Germany)
E-mail: borje@infu.uni-dortmund.de

[b] Dr. J. Oxelbark, Prof. Dr. E. De Lorenzi
Department of Pharmaceutical Chemistry
University of Pavia, Via Taramelli 12
27100 Pavia (Italy)

[c] Dr. J. Courtois, Dr. A. Simanova, Dr. J. Verhage, Prof. K. Irgum
Department of Chemistry
Umeå University
90187 Umeå (Sweden)

[d] Dr. K. Karim
Cranfield Health
Cranfield University at Silsoe
Silsoe MK45 4DT (UK)

[e] Dr. A. J. Hall
Sunderland Pharmacy School
University of Sunderland
Sunderland SR1 3SD (UK)

Supporting information for this article is available on the WWW under http://dx.doi.org/10.1002/chem.200801046.

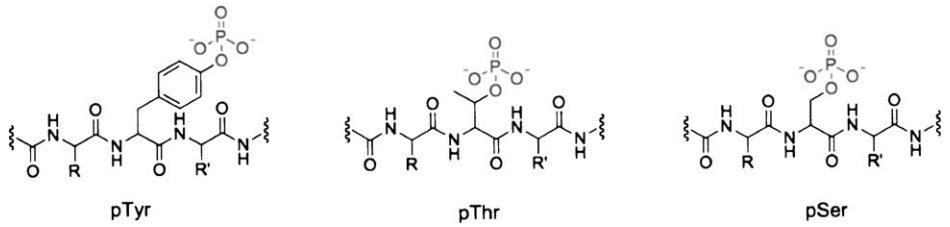

Scheme 1. The main motifs formed by post-translational phosphorylation of proteins.

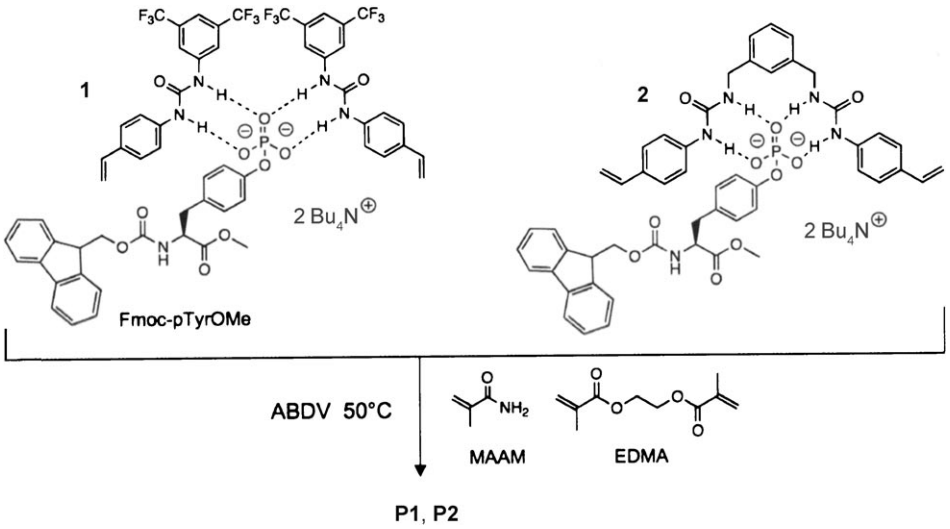

Scheme 2. Prepolymerization complexes formed between monourea monomer **1** and receptor monomer **2** with Fmoc-pTyrOMe and the procedure for the preparation of the corresponding imprinted polymers. The porogens used were THF for **P1** and DMF for **P2**.

Experimental Section

Materials: Phosphoroxytrichloride ($POCl_3$), *N*-methylmorpholine (NMM), 1-naphthyl dihydrogenphosphate (NP), tetraethylammonium tetrafluoroborate (TEATFB), trimethylolpropane trimethacrylate (TRIM), ethylene glycol dimethacrylate (EDMA), triethylamine (TEA), 2,2-diphenyl-1-picrylhydrazyl (DPPH), 1,3-bis(isocyanatemethyl)benzene, and tetrabutylammonium hydroxide (TBAOH) were Aldrich products obtained from Sigma-Aldrich (Milwaukee, USA); toluene from Fischer (Zürich, Switzerland); 1,2,2,6,6-pentamethylpiperidine, benzoin methyl ether (BME), and 3-[(methacryloyl)oxypropyl]trimethoxysilane (γ-MAPS) from Fluka (Buchs, Switzerland); *N*,*N*-dimethylformamide (DMF) from Riedel-deHaën (Seelze, Germany); 2,2′-azobisisobutyronitrile (AIBN) from SERVA (Heidelberg, Germany); acetonitrile (MeCN) and methanol from J.T. Baker (Phillipsburg, NJ, USA); *N*,*N*′-azo-bis(2,4-dimethyl)valeronitrile (ABDV) from Wako Chemicals GmbH (Neuss, Germany); 2,2,4-trimethylpentane from Merck (Darmstadt, Germany); 4-aminostyrene from Lancaster (UK); THF and dichloromethane from Acros (Geel, Belgium); and deuterated dimethyl sulfoxide ([D_6]DMSO) from Deuterio GmbH (Kastellaun, Germany).

The analytes Fmoc-pSerOH and Fmoc-pTyrOH (Fmoc = (9-fluorenylmethyl)carbamate, pSer = phosphoserine) were purchased from Bachem GmbH (Weil am Rhein, Germany); the peptide angiotensin and phosphoangiotensin from Calbiochem–Merck (Darmstadt, Germany); the zeta-chain-associated protein kinase 70 kDa (ZAP-70) peptides and reference peptides Ser-436, pSer-436, Ser-357, pSer-357, and pThr-295 (Ser = serine, pThr = phosphothreonine) were generous gifts from Prof. Rainer Bischoff (University of Groningen, Netherlands; ZAP-70) and Priv. Doz. Dr. Rainer Lehmann (University Hospital Tübingen, Germany), respectively.

EDMA was purified by the following procedure prior to use: The received material was washed consecutively with 10% aqueous NaOH, water, brine, and water. After drying over $MgSO_4$, pure dry EDMA was obtained by distillation under reduced pressure. All the other reagents were used as received. The anhydrous solvents were stored over the appropriate molecular sieves. The other solvents were of reagent grade or higher. The functional monomer *N*-3,5-bis(trifluoromethyl)-phenyl-*N*′-4-vinylphenylurea (**1**) was synthesized as reported previously.[14] The substrates Fmoc-TyrOMe, Fmoc-GluOMe, and Fmoc-LysOMe (Tyr = tyrosine, Glu = glutamic acid, Lys = lysine) were synthesized following standard procedures from the corresponding amino acid methyl esters and *N*-fluoren-9-yl methoxycarbonyloxy-succinimide.

The materials used for the MALDI-TOF mass-spectrometric analysis were as follows: Aqueous solutions were prepared using Milli-Q water filtered through a 0.2-μm membrane (Millipore). 2,5-Dihydroxybenzoic acid (DHB), α-cyano-4-hydroxycinnamic acid (CHCA), and phosphoric acid were purchased from Sigma-Aldrich (Milwaukee, USA).

Apparatus and methods: NMR spectra were recorded using a Bruker Advance DRX300 spectrometer unless otherwise stated. Elemental analysis was performed at the Department of Organic Chemistry, Johannes Gutenberg Universität (Mainz) on a Heraeus CHN rapid analyzer (Hanau, Germany). FT-IR spectroscopy was performed on a NEXUS FT-IR spectrometer (Thermo Electron Corporation, Dreieich, Germany). Nitrogen sorption measurements were performed on a Quantachrome Autosorb 6B automatic adsorption instrument (Quantachrome Corporation, Boynton Beach, FL). Prior to the measurements, samples (100–150 mg) were heated at 40–60 °C under high vacuum (10^{-5} Pa) for at least 12 h. The specific surface areas S were evaluated by using the BET method, the specific pore volumes V_p by following the Gurvitch method, and the average pore diameter D_p by using the Barrett-Joiner-Halenda (BJH) theory applied to the desorption branch of the isotherm.

Measurement of swelling: NMR tubes were filled during intermittent vibrations up to 1 cm with dry polymer particles and weighed. Solvent (1 mL) was added and the particles allowed to soak in the solvent for 24 h. The particles were then allowed to settle and the bed height of the swollen particles was measured. The swelling factor was calculated as the ratio of the bed height of the swollen particles to the bed height of the dry particles.

1,1′-[1,3-Phenylenebis(methylene)]bis[3-(4-vinylphenyl)urea] (2): 1,3-Bis(isocyanatemethyl)benzene (0.78 mL, 5 mmol) was added to a stirred solution of 4-aminostyrene (1.19 g, 10 mmol) in dry THF (40 mL) at room temperature and under a flow of nitrogen. The reaction proceeded overnight after which a white precipitate formed. The precipitate was filtered and dried under vacuum to afford the desired product as a white amorphous powder (yield: 1.49 g, 70%). ^{1}H NMR (300 MHz, [D_6]DMSO): δ = 4.25 (d, 4H), 5.05 (d, 2H), 5.61 (d, 2H), 6.59 (dd, 4H), 7.1–7.4 (m, 12H), 8.58 ppm (s, 2H); elemental analysis calcd (%) for **2**: C 73.2, H 6.14, N 13.14; found: C 72.3, H 6.0, N 13.0.

1-(4-Vinylphenyl)-3-[3,5-bis(trifluromethyl)phenyl]thiourea (3): 3,5-Bis-(trifluoromethyl)phenylisothiocyanate (3.5 mmol) was added to a stirred solution of 4-aminostyrene (3.5 mmol) in dry THF (20 mL) under nitrogen. The solution was heated to reflux overnight and then the solvent was evaporated under reduced pressure. The resulting solid residue was purified by column chromatography (silica gel, CH_2Cl_2) to give the desired product in 60% yield. ^{1}H NMR (300 MHz, [D$_6$]DMSO): $\delta = 5.22$ (d, 1H), 5.28 (d, 1H), 6.76 (dd, 1H), 7.51 (s, 4H), 7.77 (m, 1H), 8.34 (s, 2H), 9.47 (s, 1H), 9.56 ppm (s, 1H); ^{13}C NMR (300 MHz, [D$_6$]DMSO): $\delta =$ 114.21, 117.18, 122.22, 123.7, 124.13, 124.24, 124.94, 126.87, 129.85, 130.17, 130.50, 130.82, 134.37, 136.33, 138.44, 142.04, 179.81 ppm; FAB MS: m/z: 390.0 [M^+], 391.0 [M+H]$^+$; elemental analysis calcd for $C_{17}H_{12}F_6N_2S$: C 52.31, H 3.10, N 7.18, S 8.21; found: C 52.19, H 3.14, N 7.22, S 8.25.

***N*-(9-Fluorenylmethoxycarbonyl)-*O'*-phosphonotyrosine methyl ester (Fmoc-pTyrOMe)**: The synthesis of Fmoc-pTyrOMe followed a previously reported procedure starting from Fmoc-TyrOMe.[16] $POCl_3$ (1.34 mL, 14.4 mmol) and NMM (0.95 mL, 8.6 mmol) were added to Fmoc-TyrOMe (3.00 g, 7.2 mmol) in dry dichloromethane (75 mL). The solution was stirred for 3 h, whereby the conversion was monitored by TLC (chloroform/acetone, 19:1). An additional portion of $POCl_3$ (0.5 mL) and NMM (0.4 mL) were added, and the solution stirred for another 4 h. The organic phase was washed with 1 N HCl (2×) and water (1×) and thereafter evaporated. The residue was taken up in acetone (20 mL), stirred for 5 min, and evaporated. This procedure was repeated three times. The product was purified twice by column chromatography (silica gel, chloroform/methanol, 9:1, 1% acetic acid) to yield 2.13 g (61.3%). The purity was estimated by reversed-phase HPLC to be approximately 95% based on peak areas (column: C-18 Luna, mobile phase: MeCN/water (50:50, v/v, 1% TEA), UV: $\lambda = 254$ nm). ^{1}H NMR (300 MHz, [D$_6$]DMSO): $\delta =$ 2.75–3.10 (m, 2H), 3.6 (s, 4H), 4.1–4.3 (m, 4H), 7.0–8.0 ppm (m, 12H); ^{31}P NMR (300 MHz, [D$_6$]DMSO): $\delta = -1.523$ ppm (s, PO_4^-); FAB MS: m/z: 496.16 [$M-$H]$^-$; elemental analysis calcd (%) for the dihydrated complex: C 56.3, H 5.29, N 2.63; found: C 56.7, H 5.15, N 2.75.

Bis(tetrabutylammonium) 1-naphtyl phosphate (TBA$_2$NP): A solution of tetrabutylammonium hydroxide in methanol (1 M, 4.46 mL, 2 equiv) was added to 1-naphtyl phosphate (0.50 g, 2.2 mmol) in dry methanol (10 mL). The reaction mixture was stirred at room temperature for 2 h. The solvent was removed under vacuum and the oily residue dried over P_2O_5. The bis(tetrabutylammonium) salt of the template Fmoc-pTyrOMe was synthesized in a similar manner.

Tetrabutylammonium hydrogen-1-naphtyl phosphate (TBAHNP): A solution of tetrabutylammonium hydroxide (1 M, 2.2 mL, 1 equiv) in methanol was added to 1-naphthyl phosphate (0.50 g, 2.2 mmol) in dry methanol (10 mL) and the resulting solution was stirred at room temperature for 2 h. The solvent was removed and the residue dried over P_2O_5 to give a light-brown solid.

^{1}H NMR spectroscopic titrations and estimation of the complex stoichiometries and association constants: The complex stoichiometry was first assessed using the Job method of continuous variation. Stock solutions of the host monomer and guest (2 mM in [D$_6$]DMSO, respectively) were combined in NMR tubes, thereby resulting in the following molar ratios: 0:10, 2:8, 3:7, 4:6, 5:5, 6:4, 7:3, 8:2, 10:0 M. NMR spectra were thereafter recorded and the proton signals, which could be monitored for all the mixing ratios, were used for the evaluation of the complex stoichiometry.

All ^{1}H NMR spectroscopic titrations were performed in dry deuterated solvents. The association constants K for the interaction between the hosts and guests were determined by titrating an increasing amount of guest (e.g., TBAHNP) into a constant amount of functional monomer (i.e., **1** or **2**). The concentration of the functional monomer was 1 mM and the amount of added guest was 0, 0.25, 0.5, 0.75, 1.0, 1.5, 2.0, 4.0, 6.0, and 10.0 equivalents. The complexation induced shifts (CISs) of the host urea or vinyl protons were followed and titration curves were constructed of CIS versus guest concentration. The raw titration data were fitted to a 1:1 binding isotherm by nonlinear regression using Microcal Origin 5.0, from which the association constants were calculated.

Modeling: The workstation used to simulate monomer/template interactions was a Silicon Graphics Octane with the IRIX 6.5 operating system. The workstation was configured with two 195-MHz reduced instruction set processors, 2-GB memory, and a 20-GB fixed drive. This system was used to execute the software packages SYBYL 7.0 (Tripos Inc., St. Louis, Missouri, USA). The molecular model of monomer/template (dianion) complexes were minimized by using Tripos Force Fields, Gasteiger—Hückel charges, and the Powell minimization method and refined with the molecular mechanics method by applying an energy minimization with the MAXIMIN2 command. Energy minimization was performed on the monomer/template complexes to a value of 0.001 kcal mol^{-1}, and these complexes were then used for calculating the binding energy of complexation of the template to the monomers by using a computational docking program FlexiDock. The energy calculations were made based on a site-point matching score and the resulting energies cannot be equated with interaction enthalpies.

Polymer preparation

Crushed monoliths: Imprinted polymers **P1** and **P2** were prepared in the following manner: The bis(tetrabutylammonium) salt of Fmoc-pTyrOMe (template; 0.5 mmol), urea monomer (**P1**: 1 mmol **1**; **P2**: 0.5 mmol **2**), methacrylamide (4 mmol), and EDMA (20 mmol) were dissolved in THF for **P1** or DMF for **P2** (5.6 mL). The initiator ABDV (1% w/w of total monomer) was added to the solution. The solution was transferred to a glass ampoule, cooled to 0 °C, and purged with a flow of dry nitrogen for 10 min. The tubes were then flame-sealed while still cooling, and the polymerization initiated by placing the tubes in a thermostatted water bath preset at 50 °C. The tubes were broken after 24 h and the polymers lightly crushed. They were washed thereafter with MeOH/0.1 N HCl (1:1, 3×), and extracted in a Soxhlet apparatus with methanol for 24 h. This process was followed by further crushing and sieving, whereby the fraction of 25–36 μm was used for packing the HPLC columns to evaluate the binding properties. Nonimprinted polymers (**P$_N$1** or **P$_N$2**) were prepared in the same manner described above, but with the omission of the template molecule from the prepolymerization solution.

Capillary monolithic supports: Polyimide-coated capillaries of 250 μm i.d. and 360 μm o.d. were obtained from Polymicro Technologies (Phoenix, Arizona, USA). These capillaries were pretreated according a procedure based on our previous study.[17] The capillaries were washed with acetone and deionized water, flushed for approximately 5 min with 1 M aqueous NaOH, sealed in the filled state, etched by heating in a circulating air oven at 120 °C for 2 h, and cooled to room temperature. A washing procedure of deionized water and acetone (15 min each in sequence) was employed and the final drying took place in a vacuum oven at 60 °C for at least 1 h. A silanization reaction to introduce methacrylic anchoring groups onto the surface was carried out by filling the capillary with a mixture of γ-MAPS in DMF (1:1, v/v) containing 0.01% DPPH. The capillaries were sealed as above and heated at 120 °C for 6 h. Finally, the capillaries were washed with acetone and dried in a vacuum oven at 60 °C for at least 3 h.

A polymeric capillary core monolith was prepared in situ in a 2-m pretreated capillary with a solution of TRIM (40%, w/w) in a mixture of 2,2,4-trimethylpentane/toluene (70:30, w/w) as the porogen[18] and AIBN (1% with respect to the weight of TRIM) as the initiator for thermal polymerization, which proceeded for 24 h at 60 °C. This capillary core monolith was scored and snapped into 70-mm long pieces, which were individually subjected to intensive cleaning (>30 column volumes) with methanol on a Shimadzu model LC-10ADVP HPLC pump (Kyoto, Japan) with the microstepping option running at 10 μL min^{-1}. The capillaries were ranked by their back pressure as measured by the HPLC system during the washing step, and only columns that showed a constant back pressure of 3.7–3.9 MPa were selected for the grafting step. On each of these capillary core monolith columns, a UV transparent window was then made by removing 40 mm of the polyimide coating in the central part of the column with a scalpel, thus leaving 15 mm on each side to allow fitting of the column with fittings and sleeves, obtained from Upchurch Scientific (Oak Harbor, WA, USA).

Grafting of the imprinted polymer to capillary monolithic supports: The prepolymerizaton mixture was prepared as follows: The template Fmoc-pTyrOMe (≈2 mg) was mixed with the strong, non-nucleophilic base 1,2,2,6,6-pentamethylpiperidine[19] (2 equiv) to form the ionized template. The grafting solution was then prepared by mixing the template (T), urea

monomer 1, and EDMA in acetonitrile (T/1/EDMA = 1:4:40) to make up a 12% (w/w) monomer solution, and AIBN (1% w/w with respect to the combined monomer weight) was finally added as the initiator. This solution was introduced in an empty fused-silica capillary (1 m × 250 μm i.d.) and methanol was propelled by an HPLC pump to force the solution into each 70-mm column. After 10 column volumes had been pumped through the column, the column was sealed at both ends by GC septa and photografting was carried out in a UV Spectrolinker XL-1500 (Spectronics Corporation, Westbury, NY, USA) at $\lambda = 365$ nm to establish the imprinted polymer layer. The temperature inside the photografting chamber was kept at (-10 ± 3) °C, and the light intensity in the polymerization zone was 3.3 mW cm^{-2}, as determined by an International Light Model IL1400 radiometer with a model XRL140B probe (Newburyport, MA, USA). After the polymerization was completed, a 1-mm piece was trimmed from each capillary end, and thereafter the capillaries were individually flushed by at least 30 column volumes of methanol at 10 μL min^{-1}. The back pressure was measured again during the washing step, and columns that did not show an increase in the back pressure of (0.4 ± 0.1) MPa were discarded. The nonimprinted reference polymers were prepared in the same way, but the template complex was omitted from the grafting mixture.

HPLC evaluation: The 25—36-μm particle-size fraction was sedimented repeatedly (methanol/water, 80:20) to remove fine particles and then slurry-packed into HPLC columns (30 × 4.6 mm i.d. or 50 × 4.6 mm i.d.) using the same solvent mixture as the pushing solvent. Subsequent analyses of the polymers were performed using an Agilent HP1050 or HP1100 system equipped with a UV diode-array detector (DAD) and a workstation. Analyte detection was performed at $\lambda = 260$ and 220 nm, depending on the analyte, and a flow rate of 0.5 mL min^{-1}. The retention factor k was calculated as $k = (t - t_0/t_0)$, where t is the retention time of the analyte and t_0 is the retention time of the void marker (acetone or sodium nitrate).

Micro-LC evaluation: A micro-HPLC system (Shimadzu, Kyoto, Japan) consisting of an LC-10 ADVP pump and a SPD-10 AVP UV-detector fitted with a 35-nL cell from LC Packings (Amsterdam, The Netherlands) was used in the chromatographic evaluation with pure acetonitrile as the eluent. All the analytes were dissolved in acetonitrile and injected at room temperature using a microinjector (Upchurch, Oak Harbor, WA, USA) with a 35-nL external capillary loop and an electric actuator. The concentration of the injected analytes was set at 20 μg mL^{-1} (chosen for the best peak shape, retention properties, and detection) and special care was taken to keep this value accurate from one sample to another. Data acquisition was performed using Clarity software (DataApex, Prague, Czech Republic). All the spectra were recorded for 40 min at a flow rate of 4 μL min^{-1}. An equilibration period of 20 min was allowed between runs to decrease the amount of analyte retained on the column. As a result of peak asymmetry, the retention parameters were calculated based on the center of gravity of the peaks. Peak-shape considerations were used for selecting the concentration of the injected solutions.

Frontal analysis: Frontal analysis was performed using columns (50 × 4.6 mm) packed with **P1** and $\mathbf{P_N1}$ to determine single-component adsorption isotherms. The concentration steps were assessed by using the staircase method with stock solutions of Fmoc-pTyrOMe (0.001 g L^{-1} and 0.01 g L^{-1}). Ten steps in each series (10% steps) gave 20 experimental points over a 100-fold concentration range. The step times in each series were chosen to allow complete equilibration of the mobile phase with the stationary phase. Before starting the next, higher concentration series, washing times were typically set to more than three times the equilibration time because as this procedure was shown experimentally to afford correct and reproducible breakthrough times. Staircase chromatograms were recorded at $\lambda = 210$ and 265 nm, depending on the analyte concentration, to allow a sufficient signal-to-noise ratio and ensure a linear detector response. All frontal chromatograms were evaluated using the area method[20] as implemented with a Microsoft Excel worksheet. The adsorbed amount q^* is given in Equation (1), which is adapted from the step series to staircase:

$$q^*_{n+1} = q^*_n + (C_{n+1} - C_n)F_v[t_{eq} - (t_0 - t_{ea}) - t_{ep}]/[V_c - F_v(t_0 - t_{ea})] \quad (1)$$

where C is the analyte concentration in the mobile phase, F_v is the solution flow rate, t_{eq} is the breakthrough time as determined with the area method, t_0 is the measured void time of the column, t_{ea} and t_{ep} are the extra column times from the autosampler and pump, respectively, determined by replacing the column with a zero dead volume connector (t_{ea} was determined by injecting from the autosampler and t_{ep} by running a step gradient with subsequent determination of the breakthrough times), and V_c is the geometrical volume of the column tube.

Igor Pro v.3.14 (WaveMetrics inc., Lake Oswego, OR, USA) was used for nonlinear fitting of theoretical isotherms to experimental data, and best fits were evaluated with the Fisher test.[21] The adsorption isotherm models evaluated were Langmuir [Eq. (2)], bi-Langmuir [Eq. (3)], and Freundlich [Eq. (4)] where q^* is the concentration in the stationary phase at equilibrium with concentration C and C is the concentration in the mobile phase.

$$q^* = q_s bC/(1 + bC) \quad (2)$$

$$q^* = q_{s1} b_1 C/(1 + b_1 C) + q_{s2} b_2 C/(1 + b_2 C) \quad (3)$$

$$q^* = aC^m \quad (4)$$

The Langmuir models [Eqs. (2) and (3)] assume that one [Eq. (2)] or two [Eq. (3)] distinguishable classes of sites are present on the surface, each with saturation capacity q_s and binding constant b. The Freundlich isotherm [Eq. (4)], on the other hand, assumes sites to have a Gaussian distribution of binding strengths. Herein, the width of the Gaussian distribution describes the degree of heterogeneity through the index m.

Solid-phase extraction: Solid-phase extraction (SPE) experiments were performed off-line by using HPLC columns (30 × 4.6 mm i.d.) packed with **P1** and $\mathbf{P_N1}$ and manual fraction collection at the detector outlet. The hardware consisted of an Agilent HP 1050 system equipped with a binary pump, a diode-array UV detector, and workstation. Analyte detection was performed at $\lambda = 260$ and 220 nm, depending on the analyte, and a flow rate of 0.5 mL min^{-1}. The SPE experiments comprised a 2-h conditioning step using the loading solvent A, a loading step also using the loading solvent A, and an elution step using a stronger eluent B. The loading consisted of injecting single peptides or a peptide mixture (10 μL) and passing the load solvent through the column for a given time. Either one or two fractions were collected in the load and elution steps. After each run, the columns were regenerated by continuous washing with MeOH (single peptide runs) or MeOH with 0.1% trifluoroacetic acid (TFA; peptide mixture runs) for at least 2 h. The single-peptide standards were prepared by diluting a peptide stock solution (100 μL, 1 mg mL^{-1} in Millipore water) to 1 mL with mobile phase A. The model peptide mixtures comprised either all of the nine peptides shown in Table 6 dissolved in water or a limited set of them. The non-pTyr containing peptides were present at a concentration of 11 μg mL^{-1}, whereas the pTyr peptides (pAng and pZAP-70) were present at a concentration of 11 or 0.11 μg mL^{-1}.

MALDI-TOF mass spectrometry: Mass-spectrometric analysis of the fractions collected during the SPE experiments was performed using a MALDI reflector time-of-flight mass spectrometer (Autoflex II mass spectrometer, Brucker-Daltonics GmbH, Bremen, Germany) equipped with a Scout-384 source unless otherwise stated. Ions were generated by irradiation of analyte/matrix deposits by nitrogen laser at $\lambda = 337$ nm and analyzed with an accelerating voltage of 25 kV in the reflector mode and in the positive-ion mode. Data collection, in terms of the scanning conditions and the number of scans, was performed identically for all samples unless otherwise noted. The spectra were collected by accumulating 1000 laser shots, the scanning was performed by using the RP Pepmixt Par method, and the mass spectra were analyzed with flex Control software (Brucker Daltonic FLEXControl).

The sample preparation prior to the MALDI experiments shown in Table 7 was as follows: Aliquots (0.5 mL) of the collected load and elute fractions were evaporated to dryness in a vacuum oven at room temperature. The residue was dissolved in phosphoric acid in MeOH (1.3%, 100 μL). The matrix solution was prepared by dissolving DHB (40 mg) in MeCN/water (1:1, v/v; 1 mL). The matrix solution (1 μL) and the concen-

trated SPE aliquots (1 μL) were then deposited together on the target plate by using the RP Pepmixt Par method.

Slight modifications to this procedure were introduced for the samples in given in Figures S22 and S23 in the Supporting Information. In Figure S22, the matrix solution was prepared by dissolving DHB (20 mg) in water (1 mL), whereas in Figure S23, the matrix solution was prepared by dissolving DHB (25 mg) in MeCN/water (1:1, v/v; 1 mL) containing 1% phosphoric acid. In Figure S23, 1-mL aliquots were collected and the residue was directly dissolved in the DHB matrix solution (20 μL) and a 1-μL aliquot of this matrix solution was then deposited onto the target plate.

In Figure 10, the collected fractions were directly used for MALDI analysis. Saturated matrix solutions of DHB and CHCA in MeCN/water (1:1, v/v) were prepared and used for phosphorylated and non-phosphorylated peptides, respectively. The matrix solution (1 μL) and aliquots (1 μL) of the collected fractions were subsequently deposited together onto the target plate. The MALDI analysis was in this case performed on a Voyager-DE (Applied Biosystem) instrument and by using the 1—2-k reflector method.

Results and Discussion

Monomer/template complex formation: 1,3-Disubstituted ureas have long been exploited as neutral hosts for complexing oxyanion guests.[22,23] They establish cyclic hydrogen bonds that act as a twofold donor for the acceptor (carboxylate, phosphate, or sulfonate ions). The affinity for the guest increases with the acidity of the urea protons (donor ability) and the basicity of the oxyanion (acceptor ability), but is also related to the ability of the host to self-associate (poor acceptor ability) and, hence, its solubility.[24] Commonly, thioureas are used in the host design because they are more acidic and more soluble than ureas and, thus, form stronger hydrogen bonds with a given acceptor.[23] We previously found that the polymerizable 1,3-diaryl urea **1** displayed a binding constant of approximately $K = 8800\,\text{M}^{-1}$ towards tetrabutylammonium benzoate in DMSO,[14] which is in agreement with other reported diarylurea receptors.[23] The monomers could be used to imprint carboxylates, thus resulting in polymers that recognize the guest with high affinity and selectivity in water-rich media.[13]

As a first step in our evaluation of hosts to complex the phosphate species, we decided to compare this host monomer with the supposedly more potent thiourea analogue **3**.

Monomer **3** was synthesized analogously to the urea analogue in one step by adding aminostyrene to 3,5-bis(trifluorophenyl)thiocyanate. Tetrabutylammonium hydrogen-1-naphthyl phosphate (TBAHNP) and bis(tetrabutylammonium) 1-naphtyl phosphate (TBA_2NP) were chosen as mono- and dianionic guests, respectively, thus mimicking the phenylphosphate substituent of the template Fmoc-pTyrOMe. The receptor monomer solutions (1 mM in [D_6]DMSO) were titrated with a standard solution of the anion guest in up to tenfold molar excess. Table 1 shows CISs of key protons, the corresponding binding constants (K), and the complex stoichiometries determined by the Job method of continuous variation[25] or obtained from other sources.

The titration was accompanied by pronounced downfield shifts of the urea protons together with significant shifts for all the remaining protons (see Figures S3–S7 in the Supporting Information). The signals, which could be monitored throughout the titration, were used to calculate the free and bound concentrations and if possible the association constants from the resulting binding curve obtained through nonlinear regression.

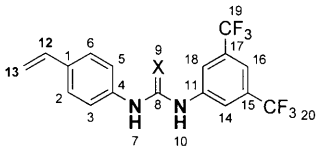

1: X=O
3: X=S

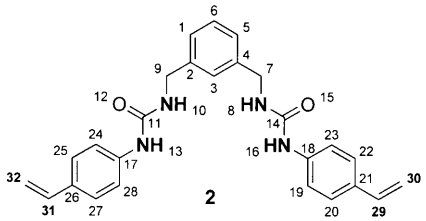

2

Table 1. Association constants, stoichiometries and CIC for complexes formed between urea host monomers and naphthyl phosphate (NP) guests in [D_6]DMSO.

Host monomer	Guest	Proton	K $\times 10^{-3}$ [M^{-1}][a]	Complex (H/G)	CIS[a] [ppm]
1	TBAHNP	NH (7,10)	2.7 ± 0.3	1:1	3.31
1	TBA_2NP	CH (13)	>10[b]	2:1	−0.14
2	TBA_2NP	CH (30,32)	>10[b]	1:1	−0.20
		NH (13,16)	n.d.		3.43
3	TBAHNP	NH (7,10)	1.1 ± 0.1	1:1	1.53
3	TBA_2NP	CH (13)	>10[b]	2:1	−0.23

[a] Average binding constants K and complexation induced shifts (CIS) based on the shift values of the resonance signals indicated. [b] A low estimate that represents the inverse of the lowest concentration of free ligand, resuling in host saturation; the two binding sites of the divalent NP was assumed to interact identically and independently with the urea host monomer **1**.

Considering first the relative complex stabilities involving monoureas **1** and **3**, the monotetrabutylammonium salt (i.e., TBAHNP) was used as a monoanionic guest to uniquely promote the formation of 1:1 complexes. After confirmation of the 1:1 stoichiometry from the Job plots, the 1:1 binding model was used to determine the respective association constants. Surprisingly, the oxourea monomer formed the most stable complexes ($K = 2675\,\text{M}^{-1}$), which were more than twofold stronger than the corresponding thiourea complexes ($K = 1089\,\text{M}^{-1}$). This behavior obviously contrasts with most previous findings on thiourea/oxyanion complexes but agrees with a recent report by Roussel et al.[26] These authors attributed the effect to a preference of the diarylthiourea species for an *E,Z* conformation in contrast to the preference of the oxyurea for a *Z,Z* conformation.

We then went on to assess the urea receptor monomer **2**, an analogue of receptors that were used previously as phosphate receptors.[27] As **2** was designed to complex the dia-

nion in a 1:1 stoichiometry, we tested its ability to complex TBA_2NP. Because of difficulties in removing the residual methanol from TBA_2NP, the urea protons could not be clearly distinguished throughout the titration, although the maximum shifts (i.e., CIS) were in agreement with reported values for similar hosts.[23] The vinyl protons, however, leveled off at a 1:1 host/guest stoichiometry (Figure 1) and the very low free concentrations allowed only a minimum value of K to be estimated as $10000\,M^{-1}$.

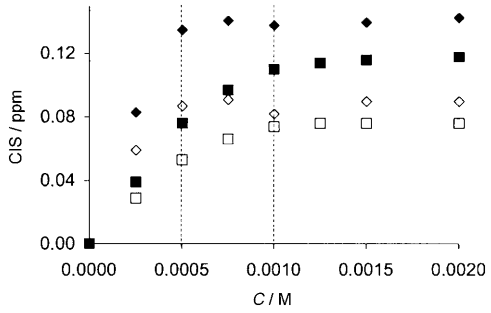

Figure 1. CIS of ($\mathbf{H}_2C=$) (solid symbols), and (=C**H**−) (open symbols) of **1** (diamonds) and **2** (squares) as a function of the total concentration C of the guest TBA_2NP in [D_6]DMSO. The dashed lines indicate the guest concentrations that correspond to 2:1 (left line) and 1:1 (right line) host/guest stoichiometries.

Probing the interactions between the monoureas and the phosphate dianion in contrast showed the vinyl protons to level off at a 2:1 host/guest stoichiometry. Although in this case as well, only a minimum value of K could be estimated, the steepness of the CIS curves indicate that the complexes are stronger in this case with the complex involving oxourea analogue **1** appearing somewhat more stable than that of the thiourea derivative **3**, the latter displaying a somewhat shallower curve.[28]

We were still puzzled about the strong complexation tendency of the monoureas, especially with respect to the bis-urea receptor monomer. In spite of the presumed ability of the bis-urea to donate four converging hydrogen bonds to the phosphate dianion guest, it displayed weaker complexes. Further insight into the origin of these differences was obtained by molecular modeling.

Molecular modeling of the host–guest complexes was performed using the genetic algorithm-based FlexiDock program for docking ligands into receptor active sites. This program works on a receptor–ligand pair in which the receptor backbone atoms are fixed in space, but the ligand is mobile (rotation/translation can be applied). The modeling gave minimum-energy complex geometries and their relative interaction energies with the latter lacking physical meaning being used for ranking purposes only. The lowest-energy complex for Fmoc-pTyrOMe and **1** (Figure 2A), with an interaction energy of $-544\,kcal\,mol^{-1}$, features the bis(trifluoromethyl)phenyl substituents of both urea ligands pointing in the same direction, thus allowing four strong hydrogen bonds to develop, and the styryl substituent of one of the ligands placed at π-stacking distance from the tyrosine phenyl group. This arrangement should result in a tight cavity complementary to the phenylphosphate group of pTyr. Conversely, the corresponding complex with **2** (Figure 2B) is poorly defined, thus resulting in an interaction energy of only $-252\,kcal\,mol^{-1}$. The orientation prevents the engagement of all the urea protons in hydrogen bonding with the phosphate group. Although the computational approach has arguable limitations, the relative interaction energies of the two complexes are interestingly in agreement with both the titration data (see above) and the affinities exhibited by the corresponding imprinted polymers (see below).

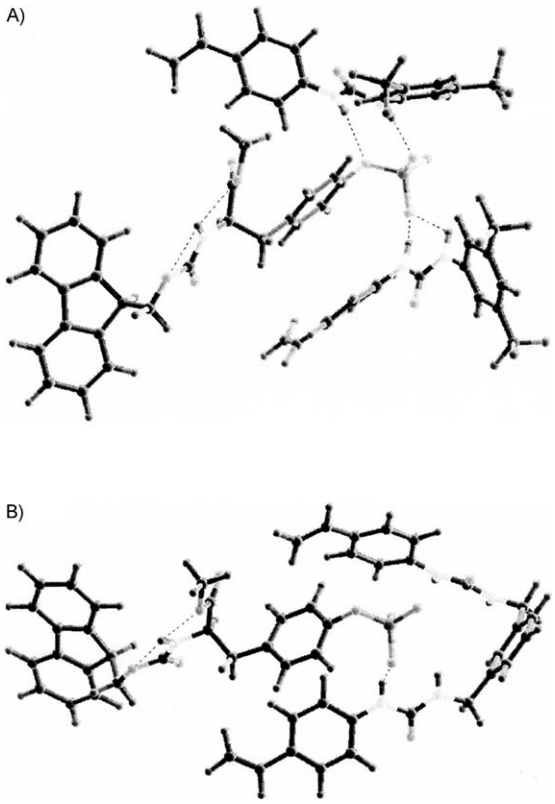

Figure 2. Ball-and-stick models of the minimum-energy complexes formed between urea monomers **1** (A) and **2** (B) with Fmoc-pTyrOMe. A) The interaction energy for the complex was $-544\,kcal\,mol^{-1}$; the hydrogen-bond lengths for the phosphate–urea interactions were 1.915 and 2.250 Å (top monomer) and 1.916 and 1.925 Å (bottom monomer); the shortest carbon–carbon distance between the pTyr phenyl ring and the phenyl ring of the bottom monomer was 3.440 Å. B) The interaction energy for the complex was $-252\,kcal\,mol^{-1}$; only one single intermolecular hydrogen bond was indicated with a length of 2.651 Å.

Polymer preparation: Having established the potency of the urea monomers **1** and **2** to complex phosphates, we turned our attention to the polymer preparation. Polymers **P1** and **P2** were prepared using monomers **1** and **2** in 2:1 and 1:1 stoichiometric ratios, respectively, to the template Fmoc-pTyr-OMe (Scheme 2). Nonimprinted polymers $\mathbf{P_N1}$ and $\mathbf{P_N2}$ were prepared identically to the imprinted polymers but with the template omitted. Methacrylamide was added as a supplementary monomer to provide additional hydro-

gen-bond stabilization[13] and EDMA as a crosslinking monomer with THF or DMF as the solvents for **P1** and **P2**, respectively. The choice of solvent was guided by the solubility of the urea/template complex in the monomer mixture. Conventional azo-initiated thermal polymerization at 50 °C subsequently afforded the imprinted and nonimprinted polymers. The polymers were crushed and sieved to a 25—36-μm particle-size fraction and subjected to template removal by washing with acidic methanol, followed by extraction with methanol in a Soxhlet apparatus. On the basis of the elemental analysis of the remaining phosphorous atoms in the polymers, more than 95% of the template was removed by this treatment.

To investigate whether the imprinted and control polymers were otherwise comparable in terms of morphology and composition, the polymers were characterized by using elemental analysis, X-ray photoelectron spectroscopy (XPS), IR spectroscopy, cross-polarization/magic-angle-spinning (CP-MAS) ^{13}C NMR spectroscopy, and nitrogen sorption analysis (see the Supporting Information). Only the nitrogen sorption technique, which shows the porous properties of the materials, and associated swelling tests gave evidence toward the differences between the imprinted and nonimprinted polymers (Table 2). Thus, all the polymers except **P1** exhibited mesoporous morphology with surface areas larger than 200 $m^2 g^{-1}$ and average pore diameters of roughly 4 nm. This finding contrasted with **P1**, which showed a lower surface area and pore volume, but on the other hand exhibited a higher swelling factor than the other materials.

Table 2. Physical properties of Fmoc-pTyrOMe imprinted and nonimprinted polymers.[a]

Polymer	S [$m^2 g$]	V_p [$mL g^{-1}$]	D_p [nm]	Swelling [$mL mL^{-1}$]
P1	70	0.076	5.3	1.9
P_N1	247	0.24	4.3	1.2
P2	208	0.22	3.8	1.8
P_N2	342	0.66	3.8	1.9

[a] The Brunauer–Emmett–Teller (BET) specific surface area S, specific pore volume V_p, and average pore diameter D_p were calculated from the nitrogen adsorption isotherms, whereas the swelling in $mL mL^{-1}$ was determined by soaking 1 mL of a packed bed of polymer particles in MeCN/water 90:10 (v/v) +1% TEA) as described in the Experimental Section.

Morphological differences induced by the template molecules are frequently reported for studies on imprinting but these differences may go in different directions, that is, resulting in polymers with either higher or lower surface areas.[29–31] This behavior is particularly true in noncovalent imprinting, in which the template may exert a complex effect that influences the solvation of the growing chains and reactivity ratios. Moreover, crosslinking levels may be influenced by divalent templates capable of complexing two monomersin different opolymer chains. Given the 2:1 stoichiometry of the urea/template complex, the latter effect is a plausible cause of morphological differences but not in the order observed herein. However, if the template acts as a solvating agent for the growing chains, the phase separation would be delayed, which in turn would lead to a polymer with a more gel-like morphology.[32] This latter explanation would be in better agreement with the observed differences between the polymers (Table 2).

Chromatographic characterization: Imprinting effects were assessed by chromatography by using the crushed polymer monoliths as the stationary phase. Our first goal was to investigate how well the polymers discriminated the template from other amino acid derivatives that contained side chains with an expected affinity for the urea motif.

Thus, Fmoc amino acid methyl esters were injected onto the columns in an acetonitrile-rich mobile phase buffered with triethylamine (Figure 3). Basic conditions were used to promote deprotonation of the template and other analytes, thus allowing more stable quadruple hydrogen bonds to develop.[14] Figure 3 shows that **P1** and **P2** exhibited a strong affinity for the template Fmoc-pTyrOMe, but that the other amino acids were only weakly retained. Polymers **P_N1** and **P_N2**, on the other hand, exhibited no affinity for any of the analytes under these conditions. Polymer **P1** exhibited stronger template retentitivity than **P2**, and this difference was magnified when assessing the polymers in a competitive phosphate-buffered mobile phase. Here, only **P1** retained the template, whereas breakthrough was seen on **P2** (see Figure S16 in the Supporting Information). The fact that **P1** still retains the template to a significant extent reflects the tight complex formed between **1** and Fmoc-pTyrOMe (see above). This result also corroborates the relative stabilities of the complexes obtained from the NMR spectroscopic titrations (Table 1) and the modeling results (Figure 2), with reservation for the somewhat more competitive solvent used when preparing **P2**.

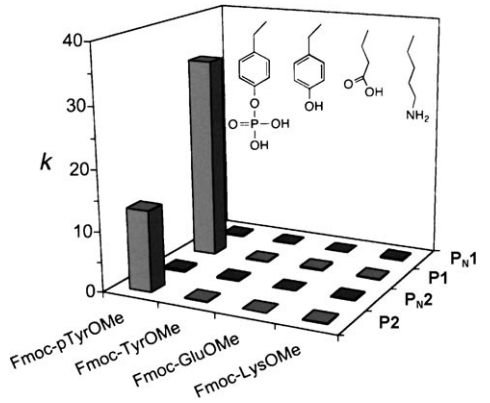

Figure 3. Chromatographic characterization of the imprinted polymers using amino acid derivatives as test solutes. Retention factors for the amino acid analytes on columns packed with the imprinted and nonimprinted control polymers. The mobile phase for **P1** and **P_N1** was: MeCN/water 90:10 (v/v) 1% triethylamine), whereas for **P2** and **P_N2** it was: MeCN/water 93:7 (v/v) 1% triethylamine.

Micro-liquid chromatography: Micro-liquid chromatography (micro-LC) using capillary-column formats is an attractive technique for separation problems that require low sample loads and mass-spectrometric interfacing.[5] These needs apply in the proteomics area in which sample volumes are strongly limited but the demand for detection sensitivity and selectivity is high. To shrink the imprinted polymers to match the micro-LC format, we used our recently reported technique based on grafting imprinted polymer layers onto flow-through poly(TRIM) monoliths with unreacted surface double bonds as anchor points.[33] Thus, imprinted and nonimprinted capillaries were prepared and subsequently assessed in the micro-LC mode. Figure 4 shows the elution profiles obtained after separate injections of the amino acid analytes with an acetonitrile-rich mobile phase modified with a cationic ion-pair reagent (IPR).

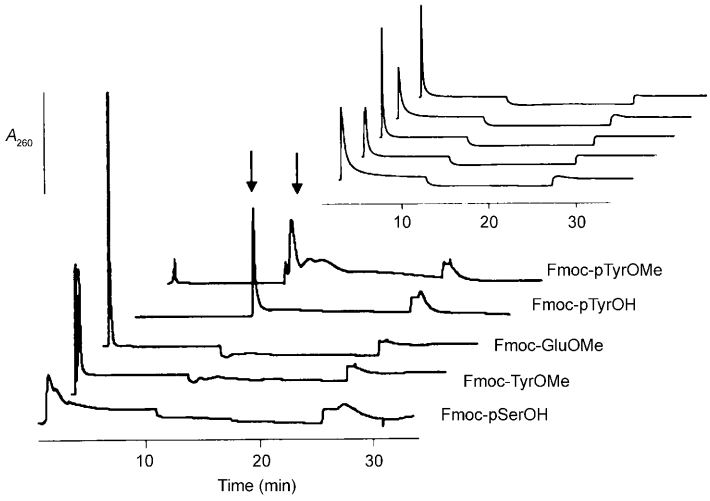

Figure 4. Micro-LC of amino acid analytes using poly(TRIM) capillaries coated with Fmoc-pTyrOMe imprinted and nonimprinted (inset) polymers. Mobile-phase A: MeCN/water 90:10 (v/v) 120 ppm tetraethylammonium tetrafluoroborate for 10 min; mobile-phase B: MeOH for 15 min; mobile-phase A for 10 min. Arrows indicate elution of pTyr analytes.

The high affinity and selectivity displayed by the imprinted polymer was also confirmed by using this format, and strong eluents were required to elute the pTyr analytes. This procedure resulted in clearly eluting peaks only for runs involving pTyr analytes on **P1**, with the notable absence of an elution peak for pSer. Thus, whereas the polymer fully retains the pTyr derivative, most of the pSer analogue breaks through within 10 minutes. In contrast to the imprinted capillary, the control capillary was incapable of retaining any of the analytes. Another encouraging point was the observed robustness of the phases and their preparation, which is reflected in the almost identical retention factors measured for multiple runs on several independently prepared imprinted capillaries (see Figure S17 in the Supporting Information).

Mobile-phase dependence: To investigate whether the retention behavior prevailed in water-rich mobile phases, the retention of the phosphorylated analytes was measured in mobile phases with different water contents (Figure 5). Plotting the retention factor versus the water content resulted in the typical bell-shaped curves observed for several imprinted polymer systems. This result is explained by a change in the retention mode from an electrostatically driven mode in water-poor systems to a desolvation (hydrophobic) retention mode at higher water contents. It can be seen that both effects contain a strong selective contribution. Thus, both pTyr-containing analytes are strongly retained at both low and high water contents, whereas pSer is only retained in the water-poor system. However, the addition of an IPR to the water-poor mobile phase reveals a selectivity for pTyr over pSer in this system too (Table 3).

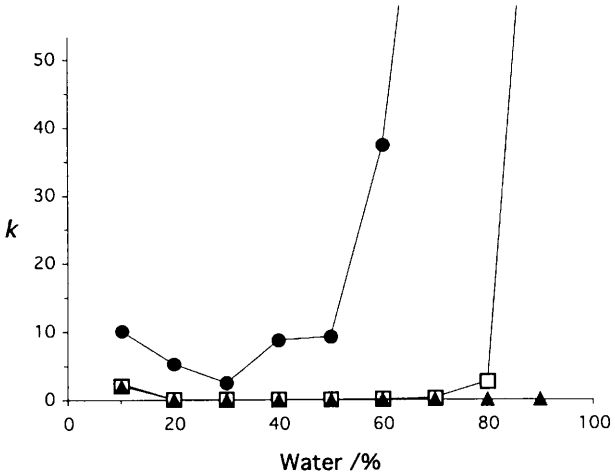

Figure 5. Retention factors in micro-LC for the amino acid analytes Fmoc-pTyrOMe (solid circles), Fmoc-pTyrOH (open squares), and Fmoc-pSerOH (solid triangles) on an imprinted polymer capillary as a function of the water content in acetonitrile/water mobile-phase mixtures. A retention factor of >50 implies that no peaks were observed within the 30-min runtime. Conditions: flow-rate $=5\,\mu L\,min^{-1}$, column dimension $=4\,cm\times320\,\mu m$ i.d.; injections $=100\,mg\,L^{-1}$ in a 180-nL loop. The column was regenerated with MeOH between each run.

Considering that the IPR had essentially no effect on the retention on the nonimprinted control polymer, this interesting behavior suggests that the IPR facilitates the access to or cobinds with the template in the imprinted sites. The results shown in Figure 6 support this hypothesis. Thus, whereas the addition of the template identical tetrabutylammonium IPR causes a strong increase in retention of Fmoc-pTyr-OMe, a more modest effect was observed upon the addition of the less complementary tetraethylammonium IPR (Figure 6, inset). Thus, the polymers exhibit a memory effect not only for the hydrogen-bonded ligand but also for the bulky countercation (Scheme 3).

Other mobile-phase compositions also resulted in strong imprinting effects (see the Supporting Information). For instance, a water-rich mobile phase (80% water) gave stron-

Table 3. Retention factors for phosphorylated amino acid analytes on a Fmoc-pTyrOMe imprinted capillary as a function of the ion pair reagent concentration in MeCN/water: 80/20 (v/v).[a]

[TEATFB] [mg L^{-1}]	k (Fmoc-pTyrOMe)	k (Fmoc-pTyrOH)	k (Fmoc-pSerOH)
0	5.3	0.11	0.07
0.25	18	0.19	0.09
50	no elution[b]	0.50	–
100	no elution[b]	0.99	0.11
215[c]	no elution[b]	3.05	0.11

[a] Conditions: flow-rate = 5 μL min^{-1}, column = 4 cm imprinted polymer capillary column (320 μm i.d.), injection: 100 mg L^{-1} of indicated solutes in a 180-nL loop; conditioning was performed with MeOH between each run. [b] No peak observed within 30 min. [c] Equal to 1 mM.

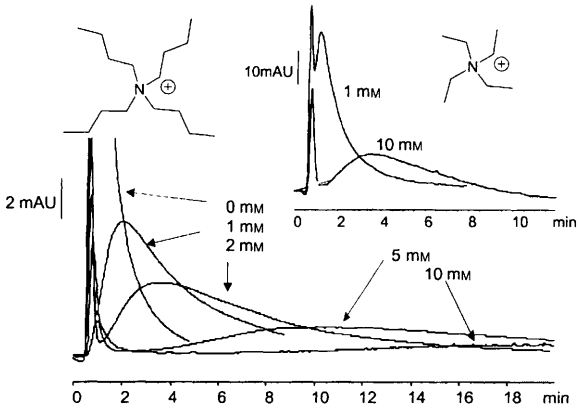

Figure 6. Elution profiles of Fmoc-pTyrOMe on **P1** as a function of the IPR concentration. Tetrabutylammonium hydroxide (TBAOH) was added to the mobile phase consisting of MeCN and sodium carbonate buffer (10 mM, pH 9.8) in a ratio of 50:50 (v/v) to reach the final concentrations indicated. Inset: the same experiment but with tetraethylammonium tetrafluoroborate (TEATFB) as the IPR. Conditions: column = 50 × 4.6 mm, DAD λ = 260, 210 nm, flow-rate = 0.5 mL min^{-1}, injection = 5 μL of 0.2 mM stock solutions in acetonitrile.

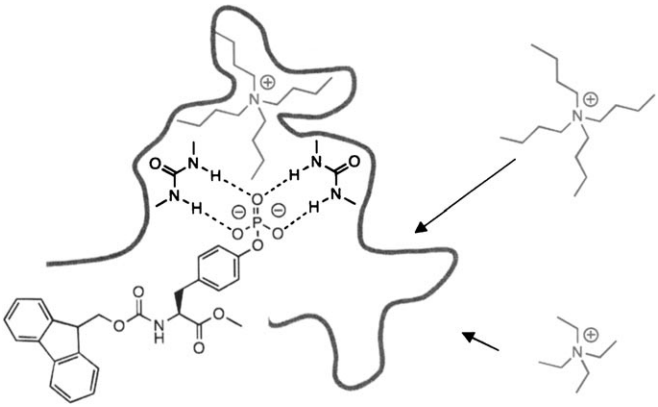

Scheme 3. A possible binding site resulting from ternary complex imprinting.

ger imprinting effects when buffered at high pH, thus again providing stronger quadruple hydrogen-bond formation. The retention effects observed under acidic conditions in the presence of 0.1% TFA as a modifier may be less expected. However, the pH value of 0.1% TFA (aqueous) is 1.9, which is slightly higher than the pK_a of a phosphate monoester (pK_a = 1.1).[3] With a charge of almost −1, the phosphate analytes are still expected to interact strongly with the imprinted receptor. This expectation was supported by FlexiDock modeling of the phosphate monoanion bound to the receptor optimized for binding the dianion. The binding energies (ca. 250 kcal mol^{-1}) were similar to those obtained for the dianion binding to the bis(urea) receptor.

Frontal analysis: The binding-energy distribution of the polymers was obtained from single-component adsorption isotherms determined by staircase frontal analysis.[34] Thus, the isotherms of Fmoc-pTyrOMe on **P1** and **P$_N$1** (Figure 7) were obtained by using the three different mobile phases that produced the zonal elution profiles shown in Figure 6 and Figure S18 in the Supporting Information.

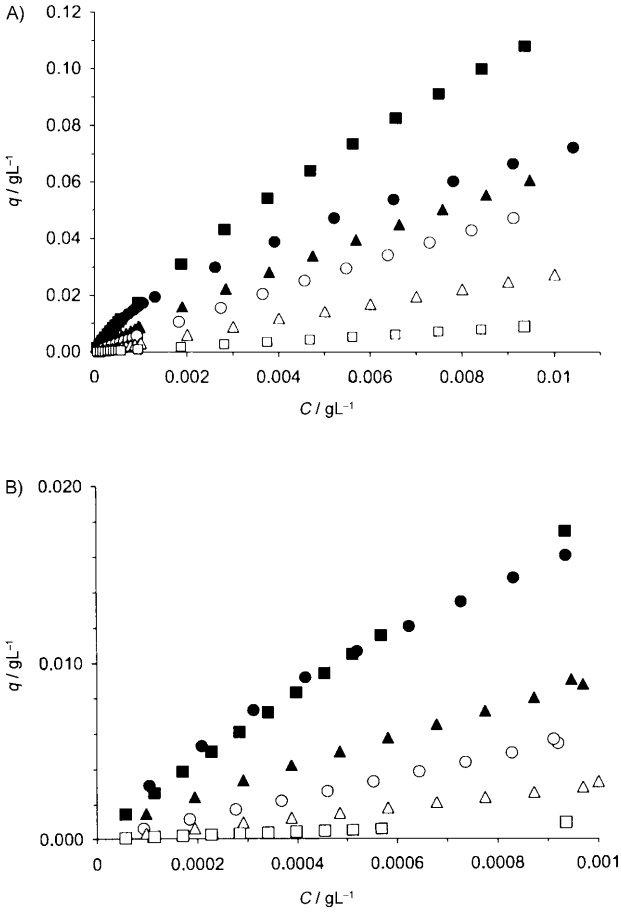

Figure 7. Adsorption isotherms obtained by frontal analysis chromatography of Fmoc-pTyrOMe on **P1** (filled symbols) and **P$_N$1** (open symbols) using mobile phase A: MeCN/(sodium carbonate buffer (0.01 M), TBAOH (0.01 M), pH 9.8) 50:50 (v/v) (squares); B: MeCN/(sodium carbonate buffer (0.01 M), pH 9.8) 20:80 (v/v) (circles); C: MeCN/water 50:50 (v/v) 0.1% TFA (triangles). A and B show all isotherms within two different concentration intervals. C = concentration in the mobile phase, q = concentration in the stationary phase.

The isotherms of **P1** exhibited clear curvature in the low-concentration range, whereas an almost linear increase in the adsorbed amount q with solute concentration C was observed at higher loads. The isotherms of $\mathbf{P_N1}$ appeared linear throughout the concentration range investigated with slopes that appeared highest when using the basic mobile phase B, followed by the acidic mobile phase C and the IPR-modified mobile phase A. This finding reflects a decrease in the nonspecific contribution to binding in the same order. Interestingly, the slopes of the same portions of the **P1** isotherms showed a different order.

Here, mobile phase A gave the highest slope, followed by B, and finally C, the latter difference becoming particularly apparent in the low-concentration interval. By using the IPR-modified mobile phase A, the end result is, thus, a strong imprint-related capacity increase. This finding again suggests that both template components used in the imprinting step are required for efficient access to the imprinted sites (Scheme 3).

The isotherms were subsequently fitted to mono-Langmuir, bi-Langmuir, and Freundlich isotherm models[35] and resulted in the isotherm parameters given in Table 4 and Table 5. All the isotherms obtained from $\mathbf{P_N1}$ were fitted with the mono-Langmuir isotherm model, but the weak curvature strongly decreases the accuracy of the derived parameters. This behavior is not the case for **P1**, which showed good fits to both the Freundlich and bi-Langmuir models depending on the mobile phase used. The parameters derived from the bi-Langmuir fittings are given in Table 4 from which we discern one class of high-energy binding sites with binding constants of 10^5–$10^6\,\text{M}^{-1}$, which are 10–100 times less abundant than lower affinity sites in the $K = 10^4\,\text{M}^{-1}$ range. It can further be noted that the choice of the mobile phase influences the relative abundance of these sites more than their associated binding constants, which agrees with the above observations.

The Fisher values in Table 5 reflect which of the models provides the best fit to a particular isotherm, a higher number, thus indicating a better fit. For instance, the isotherm obtained by using the acidic mobile phase C shows a stronger adherence to a Freundlich model. This behavior contrasts with the isotherm obtained by using the IPR mobile phase A, in which a much higher Fisher value (i.e., 64000) was obtained from the bi-Langmuir fitting. This finding may indicate that the IPR-modified phase decreases the binding-site heterogeneity of the MIPs, at least in the low-sample-load regime that is probed here.

Table 4. Parameters derived from fitting of the frontal analysis binding isotherms with Langmuir models.[a]

Polymer	Mobile phase[b]	qs_1 [mM]	K_1 [M^{-1}]	qs_2 [mM]	K_2 [M^{-1}]
P1	A	1.4	8.0×10^3	0.05	2.5×10^5
$\mathbf{P_N1}$	A	[c]	[c]		–
P1	B	0.5	15×10^3	0.03	7.6×10^5
$\mathbf{P_N1}$	B	0.8	8.0×10^3		–
P1	C	0.8	9.0×10^3	0.007	8.7×10^5
$\mathbf{P_N1}$	C	0.6	5.5×10^3		–

[a] The isotherms were fitted with the bi-Langmuir (**P1**) or mono-Langmuir ($\mathbf{P_N1}$) adsorption models. [b] A: MeCN/(sodium carbonate (10 mM)+TBAOH (10 mM), pH 9.8) 50:50 (v/v); B: MeCN/(sodium carbonate (10 mM), pH 9.8) 20:80 (v/v); C: MeCN/water 50:50 (v/v)+0.1% TFA. [c] No fitting possible as a result of very low curvature of the isotherm.

Table 5. Fisher values and Freundlich heterogeneity indices of the frontal analysis binding isotherms.[a]

Polymer	Mobile phase[b]	Fisher value		Heterogeneity index
		Freundlich	Langmuir	
P1	A	2100	64000	0.79
$\mathbf{P_N1}$	A	16000	14000	1.00
P1	B	7000	22000	0.64
$\mathbf{P_N1}$	B	5000	23000	0.93
P1	C	15000	10800	0.84
$\mathbf{P_N1}$	C	4900	8800	0.94

[a] The isotherms were fitted with the bi-Langmuir (**P1**) or mono-Langmuir ($\mathbf{P_N1}$) adsorption models. [b] A: MeCN/(sodium carbonate (10 mM)+TBAOH (10 mM), pH 9.8) 50:50 (v/v); B: MeCN/(sodium carbonate (10 mM), pH 9.8) 20:80 (v/v); C: MeCN/water 50:50 (v/v)+0.1% TFA.

In view of the high binding constant ($K = 7.6\times10^5\,\text{M}^{-1}$) obtained using a water-rich mobile phase (80% water), a comparison of the affinities with those observed for antibodies elicited to react with pTyr seems justified.[36] The latter exhibited binding affinities under optimal conditions that amounted to $K = 10^6$–$10^7\,\text{M}^{-1}$, thus leading to the conclusion that our synthetic receptors bind pTyr almost as strongly as their biological counterparts, albeit under different conditions.

Phosphopeptide recognition: Crucial to the utility of the reported imprinting strategy would be the extent to which these pTyr-selective sites would cross-react with peptides containing this epitope. This behavior is far from evident given the size of the template and the lack of pore-system control in conjunction with the formation of the imprinted sites. An answer to this question was provided by the use of a small set of test peptides available in the mono- and non-phosphorylated forms and including Tyr, Ser, and Thr as phosphorylation sites (Table 6).

We first investigated the retention of the stable neuropeptide angiotensin II (Ang), containing an internal tyrosine residue present in both the non-phosphorylated (Ang) and monophosphorylated (pAng) forms. To better understand the retention mechanism of these peptides, they were injected onto **P1** and $\mathbf{P_N1}$ using a series of TFA-modified binary acetonitrile/water mobile-phase mixtures. The acidic modifier TFA was anticipated to act as an anionic IPR, thus providing effective solubilization of the peptides[37] without disrupting the phosphate binding-site interactions (see above). The sometimes strong retention of the peptides (see Figure 9 and Figures S19–S20 in the Supporting Information) and their weak UV chromophores precluded accurate measurement of the retention times; therefore, we decided instead to record the portion of total peptide injected that eluted with minor retention within the first 10 min after in-

Table 6. Tyr and Ser-containing model peptides used to probe the phosphoselectivity of the polymers.[a]

Peptide	Non-phosphorylated	*m/z*	Phosphorylated	*m/z*
ZAP-70	ALGADDSYYTAR	1303	ALGADDSpYYTAR	1383
Ang	DRVYIHPF	1047	DRVpYIHPF	1127
Ser-436	CDFRSFRSVT	1305	CDFRpSFRSVT	1385
Ser-357	AHRHRGSARLHPPLNHS	1944	AHRHRGpSARLHPPLNHS	2025
pThr-295	–		SQVGLpTRRSRTE	1471

[a] The phosphorylated peptides are indicated by the letter p; for example, pAng = phosphorylated angiotensin.

jection (Figure 8A). To avoid carrying over effects from the strong retention, the columns were regenerated after each run by methanol.[38] A strong phosphopeptide preference was evident, as seen in the large difference in the percentage of eluted peptide on comparing the two peptide forms. Ang was poorly retained on both **P1** and $\mathbf{P_N1}$, except in water-rich mobile phases (>80% water), in which hydrophobic nonspecific binding becomes prevalent. pAng also breaks through completely, but only on $\mathbf{P_N1}$ and with the exception for water-poor mobile phases, in which some retention is observed. Polymer **P1** retains the phosphorylated peptide selectively and mainly in water-poor and water-rich mobile phases. An example is shown in Figure 9 of these **P1** and $\mathbf{P_N1}$ systems using a mobile phase containing 80% water. Whereas pAng appears almost quantitatively retained on **P1**, it breaks through on $\mathbf{P_N1}$. Meanwhile, Ang breaks through completely on all columns.

The results were supported by MALDI-TOF mass-spectrometric analysis of fractions collected prior to and after the switch from mobile phase A to the eluting mobile phase B (Figure 10). Here, we chose to focus on the water-poor mobile phase A (MeCN/water, 95:5), thus showing low nonspecific hydrophobic binding and high pAng selectivity. The Ang peptides exhibited minimal fragmentation in the MALDI experiment and appeared as peaks, thereby agreeing with the molecular mass of the parent peptide. This procedure allows rough estimates of the peptide contents in each fraction from the relative peak intensities to be made. As can be seen in Figure 10, the MALDI-TOF mass-spectrometric results support the UV detection results shown in Figure 8A. Thus, Ang is recovered from mobile phase A on both columns, whereas pAng is selectively retained on **P1**. This fraction can be recovered by using a somewhat stronger eluent (MeOH + 0.1% TFA), but the lower intensity of the corresponding elution peak would suggest the recovery to be incomplete. However, because MALDI can, at the most, give estimates of the relative peptide abundances, conclusions concerning the mass balance would be premature.

Having established the selectivity of **P1** for a phosphorylated versus a nonphosphorylated peptide, we turned to in-

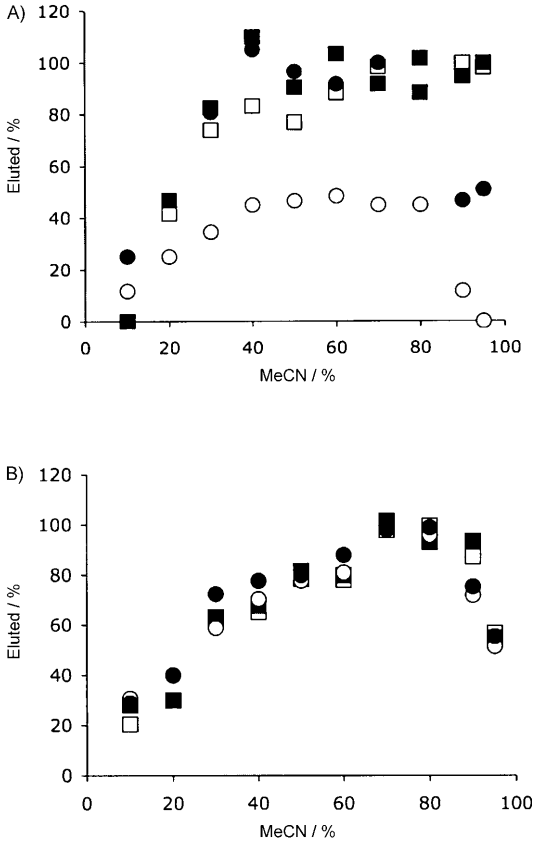

Figure 8. Results from SPE experiments of peptide analytes on **P1** and $\mathbf{P_N1}$. Effect of the MeCN/water ratio (+0.1% TFA) on the breakthrough portion (based on peak area) of A) Ang (squares) and p-Ang (circles) and B) Ser-436 (squares) and pSer-436 (circles) on **P1** (open symbols) and $\mathbf{P_N1}$ (solid symbols) within the first 10 minutes of elution. The peptides (10 μL) were injected as 0.1 mg mL^{-1} solutions in the mobile phase.

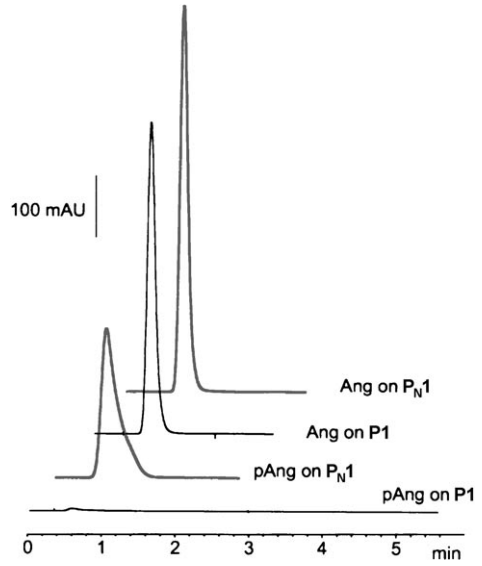

Figure 9. Elution profiles of Ang and pAng injected on **P1** and $\mathbf{P_N1}$ with MeCN/water 20:80 (v/v) 0.1% TFA as mobile phase A. Reconditioning was performed using MeOH (+0.1% TFA) as mobile phase B. Method: 0–30 min 100% A; 30–40 min 100% B. Injection: 10 μL of peptide (0.1 mg mL^{-1}) in mobile phase A; flow-rate = 0.5 mL min^{-1}, λ = 260 nm.

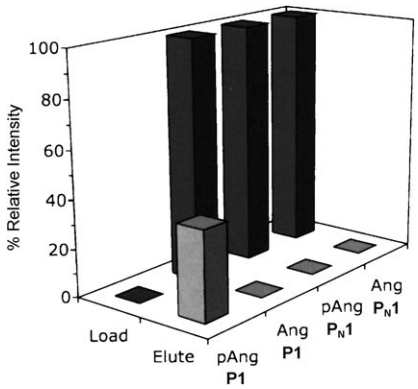

Figure 10. MALDI-TOF MS analysis of fractions collected with a 10-min interval after separate injection of Ang or pAng on **P1** or $\mathbf{P_N1}$ using the loading mobile phase A (Load) and after switching to an eluting mobile phase B (Elute). Load (A): MeCN/water 95:5 (v/v) 0.1% TFA; elute (B): MeOH + 0.1% TFA. The relative peak intensities were calculated with reference to the total peak intensity of the mass spectra. SPE method: 0–10 min 100% A; 10–20 min 100% B. Injection: 10 μL of peptide (0.1 mg mL^{-1}) in the load mobile phase A. Flow rate: 0.5 mL min^{-1}.

vestigate whether the receptors could discriminate between pTyr- and pSer-containing peptides. For this purpose, we performed measurements on the breakthrough fractions of the Ser-containing reference peptides Ser-436 and pSer-436 in analogy to the experiment performed on Ang and pAng. The results shown in Figure 8B contrast with the results obtained for the pTyr peptide Ang because no evidence for a phosphate-related selectivity was seen. Thus, Ser-436 and pSer-436 behave in a seemingly identical manner on both **P1** and $\mathbf{P_N1}$, thus generally resulting in somewhat lower recoveries at both high and low aqueous contents relative to the Ang results.

Although encouraging, the results discussed so far are based on separate injections of the peptide analytes and may not reflect the ability of the polymer to enrich phosphorylated peptides from peptide mixtures. We, therefore, performed SPE experiments that used two model peptide mixtures comprising pTyr and non-pTyr peptides present in weight ratios of 1:1 and 1:100, respectively (Table 7). Direct MALDI-TOF mass-spectrometric analysis of the load and elute fractions was performed to demonstrate the presence or absence of the peptides and to provide a rough measure of their abundance. Unfortunately, distinct peaks were displayed only for Ang and pAng, whereas the resolution and sensitivity was insufficient to clearly identify the remaining peptides. For instance, the masses of ZAP-70 and Ser-436 and their phosphorylated counterparts were within the instrument resolution, thus precluding their separate identification. On the other hand, Ser-357, pSer-357, and pThr-295 appeared with very low signal intensities and could not be identified in a reliable way.[39] To partly circumvent these problems, additional SPE experiments were performed on model peptide mixtures of decreased complexity (see Figures S22 and S23 in the Supporting Information).

Collectively, the SPE results revealed a preferential retention of pTyr-containing peptides at both spiking levels. Thus, whereas the non-phosphorylated peptides or those phosphorylated at Ser are recovered mainly in the load fractions, the pTyr peptides pAng and pZAP-70 are selectively retained by **P1**.

Conclusion

The results show that combinations of binding motifs from host–guest chemistry with conventional imprinting may be very rewarding. Thus, the stable complexes formed between the diarylurea host monomers and quaternary ammonium phosphate salts result in exceptionally tight binding sites when imprinted. With binding constants for the amino acid template exceeding $K = 10^7\,\mathrm{M}^{-1}$ in a aqueous-rich solvent (80% water), the pTyr-imprinted polymers compare favorably to pTyr antibodies, which display upper affinities in the $K = 10^6$–$10^7\,\mathrm{M}^{-1}$ range.[36] The nature of the binding site could be deduced from NMR spectroscopic titrations and molecular-modeling experiments. These data all suggested the formation of tight complexes between two diarylurea monomers and one phosphate group through quadruple hydrogen bonding possibly aided by a π–π interaction between one of the monomer ligands and the tyrosine phenyl group.

The sites exhibit sufficient binding energy to bind shorter peptides containing phosphorylated tyrosine, whereby the templating induces clear pTyr selectivity. The ability of these sites to discriminate between pSer- and pTyr-containing shorter peptides, along with the apparently small charge-dependent sequence bias, seems promising for future applications of the polymers as robust and generic pTyr-selective SPE phases. The approach also appears suited for the design of sequence specific phases, for instance, targeting disease biomarkers or for more advanced peptide fractionation.

Table 7. Peak intensities of peptides identified by MALDI-TOF mass spectrometric analysis of fractions collected during SPE experiments performed using **P1** or $\mathbf{P_N1}$.[a]

		P1				**P$_N$1**			
pY/non-pY	Peptide[b]	Load 1	Load 2	Elute 1	Elute 2	Load 1	Load 2	Elute 1	Elute 2
	Ang	2325	0	0	0	1751	0	0	0
1:1	p Ang	893	121	36	1018	5525	317	81	0
	Ser-436/ZAP-70[c]	1118	0	0	0	1009	0	0	0
	Ang	1632	0	0	0	919	0	0	0
1:100	p Ang	66	31	38	25	55	63	0	0
	Ser-436/ZAP-70[c]	1065	0	0	0	512	0	0	0

[a] The fractions were collected at 5-min intervals after injection (10 μL) of a model peptide mixture on **P1** or $\mathbf{P_N1}$ using a loading mobile phase A (Load) and afterward switching to an eluting mobile phase B (Elute). Mobile phase: 1–10 min: A = MeCN/water 95:5 (v/v) 0.1% TFA; 10–20 min: B = MeOH (0.1% TFA). [b] The peptide mixture consisted of nine peptides each at a concentration of 11 μg mL^{-1} (pY/non-pY = 1:1) or all at 11 mg mL^{-1} except for pAng and pZAP-70, which were present at a concentration of 0.11 μg mL^{-1} in water (pY/non-pY = 1:100). [c] Nonresolved peak assigned to Ser-436 and ZAP-70.

Acknowledgements

This project was financially supported by the European Community within the Human Potential Programme under the contract HPRN-CT-2002–00189 (AquaMIP). The authors are grateful to Prof. Rainer Bischoff (University of Groningen, The Netherlands) and Priv. Doz. Dr. Rainer Lehmann (University Hospital Tübingen, Germany) for valuable discussion and their generous gifts of peptides. We also wish to thank Dr. Panagiotis Manesiotis and Prof. Lihua Zhang for experimental advice and assistance.

[1] S. A. Johnson, T. Hunter, *Nat. Methods* **2005**, *2*, 17–24.
[2] B. Bodenmiller, L. N. Mueller, M. Mueller, B. Domon, R. Aebersold, *Nat. Methods* **2006**, *4*, 231–237.
[3] M. R. Larsen, T. E. Thingholm, O. N. Jensen, P. Roepsdorff, T. J. D. Jörgensen, *Molecules Molecular and Cellular Proteomics* **2005**, *4.7*, 873–886.
[4] J. Rush, A. Moritz, K. A. Lee, A. Guo, V. L. Goss, E. J. Spek, H. X. Zhang, X.-M. Zha, R. D. Polakiewicz, M. J. Comb, *Nat. Biotechnol.* **2005**, *23*, 94–101.
[5] T. Miliotis, P.-O. Ericsson, G. Marko-Varga, R. Svensson, J. Nilsson, T. Laurell, R. Bischoff, *J. Chromatogr. B* **2001**, *752*, 323–334.
[6] C. Alexander, H. S. Andersson, L. I. Andersson, R. J. Ansell, N. Kirsch, I. A. Nicholls, J. O'Mahony, M. J. Whitcombe, *J. Mol. Recognit.* **2006**, *19*, 106–180.
[7] *Molecularly Imprinted Polymers, Man-made Mimics of Antibodies and Their Applications in Analytical Chemistry* (Ed.: B. Sellergren), *Vol. 23*, Elsevier Science B.V., Amsterdam, **2001**.
[8] N. W. Turner, C. W. Jeans, K. R. Brain, C. J. Allender, V. Hlady, D. W. Britt, *Biotechnol. Prog.* **2006**, *22*, 1474–1489.
[9] A. Rachkov, N. Minoura, *Biochim. Biophys. Acta Protein Struct. Mol. Enzymol.* **2001**, *1544*, 255–266.
[10] M. M. Titirici, A. J. Hall, B. Sellergren, *Chem. Mater.* **2003**, *15*, 822–824.
[11] H. Nishino, C.-S. Huang, K. J. Shea, *Angew. Chem.* **2006**, *118*, 2452–2456; *Angew. Chem. Int. Ed.* **2006**, *45*, 2392–2396.
[12] P. Manesiotis, A. J. Hall, M. Emgenbroich, M. Quaglia, E. de Lorenzi, B. Sellergren, *Chem. Commun.* **2004**, 2278–2279.
[13] J. L. Urraca, A. J. Hall, M. C. Moreno-Bondi, B. Sellergren, *Angew. Chem.* **2006**, *118*, 5282–5285; *Angew. Chem. Int. Ed.* **2006**, *45*, 5158–5161.
[14] A. J. Hall, P. Manesiotis, M. Emgenbroich, M. Quaglia, E. De Lorenzi, B. Sellergren, *J. Org. Chem.* **2005**, *70*, 1732–1736.
[15] A. Ojida, Y. Mito-oka, K. Sada, I. Hamachi, *J. Am. Chem. Soc.* **2004**, *126*, 2454–2463.
[16] C. Krog-Jensen, *Lett. Peptide Sci.* **1999**, *6*, 193–197.
[17] J. Courtois, M. Szumski, E. Byström, A. Iwasiewicz, A. Shchukarev, K. Irgum, *J. Sep. Sci.* **2006**, *29*, 14–24.
[18] C. Viklund, K. Irgum, *Macromolecules* **2000**, *33*, 2539–2544.
[19] R. Z. Sommer, H. I. Lipp, L. L. Jackson, *J. Org. Chem.* **1971**, *36*, 824–828.
[20] G. Guiochon, S. Golshan-Shirazi, A. Katti, *Fundamentals of Preparative and Nonlinear Chromatography*, Academic Press, New York, **1994**.
[21] Y. Chen, M. Kele, I. Quinones, B. Sellergren, G. Guiochon, *J. Chromatogr.* **2001**, *927*, 1–17.
[22] E. Fan, S. A. Van Arman, S. Kincaid, A. D. Hamilton, *J. Am. Chem. Soc.* **1993**, *115*, 369–370.
[23] D. Esteban Gomez, L. Fabbrizzi, M. Licchelli, E. Monzani, *Org. Biomol. Chem.* **2005**, *3*, 1495–1500.
[24] M. C. Etter, T. W. Panunto, *J. Am. Chem. Soc.* **1988**, *110*, 5896–5897.
[25] K. A. Connors, *Binding Constants. The Measurement of Molecular Complex Stability*, Wiley, New York, **1987**.
[26] C. Roussel, M. Roman, F. Andreoli, A. Del Rio, R. Faure, *Chirality* **2006**, *18*, 762–771.
[27] P. Bühlmann, S. Nishizawa, K. P. Xiao, Y. Umezawa, *Tetrahedron* **1997**, *53*, 1647–1654.
[28] The differences between the tendency of the monomer to complex the phosphate probe became more obvious when deprotonation was attempted in situ with triethylamine as the base; on using this weaker base, ion pairing competes with urea complexation and leads to significantly weaker complexes with poorly defined stoichiometries. The relative stabilities of the monomer/phosphate complexes agreed with the slopes of the isotherms and the maximum CIS values obtained (see Figures S8–S11 in the Supporting Information).
[29] G. Wulff, *Angew. Chem.* **1995**, *107*, 1958–1979; *Angew. Chem. Int. Ed. Engl.* **1995**, *34*, 1812–1832.
[30] B. Sellergren, *J. Chromatogr. A* **1994**, *673*, 133–141.
[31] B. Sellergren, K. J. Shea, *J. Chromatogr.* **1993**, *635*, 31.
[32] This behavior agrees with the results obtained for polymers prepared in the presence of good solvents (see ref. [31]).
[33] J. Courtois, G. Fischer, B. Sellergren, K. Irgum, *J. Chromatogr. A* **2006**, *1109*, 92–99.
[34] P. Sajonz, M. Kele, G. Zhong, B. Sellergren, G. Guiochon, *J. Chromatogr.* **1998**, *810*, 1–17.
[35] K. D. Shimizu in *Molecularly Imprinted Materials: Science and Technology* (Eds.: M. Yan, O. Ramström) **2005**, pp. 419–434.
[36] S. Ruff-Jamison, R. Campos-Gonzalez, J. R. J. Glenney, *J. Biol. Chem.* **1991**, *266*, 6607–6613.
[37] D. Guo, C. T. Mant, R. S. Hodges, *J. Chromatogr.* **1987**, *386*, 205–222.
[38] The conditioning solvent and the time of column conditioning strongly influenced the retentivity of the pTyr peptides; thus, insufficient conditioning led to breakthrough of the peptides and low recovery in the elution step, whereas extensive conditioning caused a strong retentitivity (for example, see Figure 9).
[39] The serine-phosphorylated peptides exhibited limited stability in the TFA-modified eluents and partial decomposition of the samples may have occured prior to analysis.

Received: May 30, 2008
Published online: October 10, 2008

